Performance Analysis of Ultra-Wide Band Impulse Radio (UWB-IR) with Super-Orthogonal Turbo Codes (SOTC)

Usman Riaz, Man-On Pun and C.-C. Jay Kuo

***Abstract*— Low-complexity low-rate super-orthogonal turbo codes (SOTC) are proposed in this work to replace the implicit repetition code (RC) in an ultra-wide band impulse radio (UWB-IR) system to improve BER, transmission range and system throughput. Various receivers including matched-filter and RAKE receivers are adopted for data detection in the additive white Gaussian noise (AWGN) channel and the indoor IEEE 802.15.3a channel. The performance of SOTC-encoded UWB is analyzed and validated by computer simulation. It is shown that the SOTC-based UWB-IR system can achieve significant performance improvement over the conventional DS-UWB system encoded by RC.**

I. Introduction

Ultra-wide-band impulse-radio (UWB-IR) is a technique that uses very narrow low duty cycle radar-like pulses of the order of nano seconds for information transmissions [1]. The employment of these narrow pulses results in occupancy of several Giga-Hertz of bandwidth. UWB-IR can be viewed as a bandwidth unconstrained but power spectral density (PSD) constrained system. To increase the effective energy per symbol, multiple pulses (namely, N_s pulses) carrying the same information symbol are transmitted. From the coding perspective, this is equivalent to the repetition code (RC). However, a large value of N_s reduces system throughput and transmission energy efficiency per information symbol for a given pulse duration. This presents a severe problem to high-speed short-range indoor applications or low-speed long-range low-power outdoor applications such as sensor networks. In this work, we focus on the latter applications that have a strict constraint on transmission energy per symbol.

Furthermore, it is well known that increasing N_s does not provide any coding gain for RC if the SNR value (measured in terms of E_b/N_0) remains constant. Hence, more sophisticated coding schemes are desired to replace the existing RC of UWB-IR to improve system throughput, the transmission range and energy efficiency. Some efforts have been made in the past. For example, low-rate superorthogonal convolutional codes (SOCC) [2] and an adaptive combination of turbo codes and RC [3] were studied in the literature. In our previous work [4], we proposed to replace the RC of UWB-IR with the super-orthogonal turbo codes (SOTC). Being different from the conventional turbo codes that have to correlate the received sequence with all possible trellis branches, SOTC employs the inverse Walsh Hadamard Transform (IWHT) in calculating the trellis branch metrics, which results in low decoding complexity [5]. Moreover, we compared the performance of the SOTC-encoded UWB system using two types of receivers, namely, the RAKE receiver and a simple matched filter (MF) receiver, in the AWGN and the IEEE 802.15.SG3a UWB channels. The superior performance of the SOTC encoded UWB system was confirmed by computer simulation in [4]. However, theoretical analysis of the system performance was not covered in [4].

In this work, we first derive the analytical performance bounds for the SOTC-encoded UWB system. For the medium-to-high SNR range, the asymptotic performance bounds can be obtained by resorting to the effective free distance of constituent codes of SOTC. Then, since the SOTC-encoded UWB system operates primarily at the low SNR range, we use a semi-analytical method to analyze the system in IEEE 802.15.SG3a UWB channel without inter-symbol interference (ISI) at low SNR. Furthermore, we investigate the effect of N_s on system throughput, bit error probability (BEP) and the transmission range for both RC and SOTC encoded UWB-IR systems. Finally, analytical results are verified by simulation.

II. System Model

A. Signals and Channels

Similar to [4], we consider the SOTC encoded UWB-IR using DS-BPSK modulation in a single user scenario. The transmitted signal is given by

$$s(t) = \sum_{j=-\infty}^{\infty} \sqrt{E_g} \cdot b_j \cdot \sum_{i=0}^{N_s-1} a_i g(t - jT_s - iT_c), \quad (1)$$

where $E_g = \frac{E_b}{N_s}$ is the energy of the transmitted waveform with E_b being the energy per bit and $a_j \in \{-1, 1\}$ is the j-th data symbol. $a_i \in \{-1, 1\}$, $0 \le i \le N_s$, is the pseudo-random direct sequence code while $g(t)$ is a Gaussian pulse shape with $\int_{-\infty}^{\infty} g^2(t)dt = 1$. T_c and T_s are the chip and the symbol durations, respectively where T_c in the sequel is also referred to as frame duration. Since each information bit is transmitted with N_s pulses, the effective bit rate or throughput is $R_s = 1/T_s = (N_s \cdot T_c)^{-1}$.

Two channel models are considered in this work. They are the traditional AWGN and the UWB multi-path channel specified by IEEE 802.15.3a [6]. The IEEE-802.15.SG3a channel is a modified S-V model that can be written as [7]

$$h_{\text{multi-path}}(t) = X \sum_{n=1}^{N} \sum_{k=1}^{K(n)} \alpha_{n,k} \delta(t - T_n - \tau_{n,k}), \quad (2)$$

where X is the total multi-path gain and T_n is the exponentially-distributed arrival time instance of the n-th cluster. Parameters $\tau_{n,k}$ and $\alpha_{n,k}$ are the exponentially-distributed

The authors are with Department of Electrical Engineering and Signal and Image Processing Institute, University of Southern California, Los Angeles, CA 90089-2564, USA. E-mails: uriaz@usc.edu, mpun@sipi.usc.edu and cckuo@sipi.usc.edu

1-4244-0357-X/06/$20.00 ©2006 IEEE

This full text paper was peer reviewed at the direction of IEEE Communications Society subject matter experts for publication in the IEEE GLOBECOM 2006 proceedings.

arrival time instance and the amplitude of the k-th ray within the n-th cluster, respectively. $\alpha_{n,k}$ is defined as

$$\alpha_{n,k} = p_{n,k}\beta_{n,k}, \tag{3}$$

where $p_{n,k}$ is a discrete binary random variable with equally probable ± 1 and $\beta_{n,k}$ is a log-normal random variable.

To maintain the overall channel gain unity, we assume $X = 1$ and $\sum_{n,k} \alpha_{nk}^2 = 1$ in the sequel to take into account the multipath energy capture without the pathloss factor. For the IEEE-802.15.3a channel, the received signal can be written as

$$r(t) = \sum_{n=1}^{N} \sum_{k=1}^{K(n)} \alpha_{n,k} s(t - T_n - \tau_{n,k}) + v(t), \tag{4}$$

where $v(t)$ is zero-mean complex AWGN of variance σ^2.

B. Receiver Structure

Two types of receivers are considered in this work, namely, the MF-based receiver and the RAKE receiver. Among the RAKE receivers, three types of receivers are examined: All RAKE (ARAKE) that combines all the multi-paths (also referred to as ideal RAKE), Selective RAKE (SRAKE) that combines L_s paths with the strongest signal power and Partial RAKE (PRAKE) that selects the first L_p paths. The correlation mask used in the RAKE receiver can be expressed as

$$m_{\text{corr-RAKE}_j} = \sum_{l=1}^{L} \omega_l m_{corr_j}(t - \tau_l), \tag{5}$$

where $\{\tau_l; l = 1, 2, \cdots, L\}$ is a subset of path delays chosen from $\tau_{n,k}$ and ω_j is the weight for the j-th multipath. The correlation mask, $m_{corr}(t)$, is given as

$$m_{corr_j}(t) = \sqrt{E_g} \sum_{i=0}^{N_s-1} a_i g(t - jT_s - iT_c). \tag{6}$$

In this study, we consider an ISI-free IEEE-802.15.3a CM1 channel [6]. Let $s_j(t)$ is the signal corresponding to the jth information bit in (1) and $r_j(t)$ be the corresponding received signal in (4). Then, for a given multi-path delay $\tau_{L,M}$, the output of the RAKE receiver corresponding to the j-th information bit can be approximated as

$$\begin{aligned} \xi_j &= \sqrt{E_g} \cdot \sum_{i=0}^{N_s-1} \int_{iT_c}^{(i+1)T_c} r_j(t) m_{corr_j}(t - \tau_{\text{L,M}}) dt \quad (7) \\ &\approx N_s E_g b_j \alpha_{\text{LM}}^2. \quad (8) \end{aligned}$$

By capturing more multi-paths, the RAKE receiver can exploit the implicit time diversity existing in a multi-path channel.

III. Performance Analysis

We consider an SOTC scheme consisting of two recursive systematic SOCCs with primitive feedback polynomials $[1, 5]_{oct}$ that can be expressed as $G(D) = 1 + D^2$, where D isf the one-element delay of the shift register. The polynomial representation for a rate-$\frac{1}{4}$ SOCC can be determined as

$$\left[\frac{1+D^3}{1+D+D^3}, \frac{1+D^2+D^3}{1+D+D^3}, 1, \frac{1+D+D^2+D^3}{1+D+D^3}\right]. \tag{9}$$

While the performance of RC is determined by its free distance, $d_{\text{free-RC}}$ with BEP of $Q\left(\sqrt{2N_s\frac{E_g}{N_0}}\right)$, the asymptotic performance of SOTC with uniform interleaver analysis depends on the *effective* free distance of its constituent SOCC, $d_{\text{free-eff}}$ [8]. In the following, we first derive the effective free distance of the constituent SOCC based on minimum weight $w_{min} = 2$. Then, the resulting $d_{\text{free-eff}}$ is exploited to obtain the asymptotic performance of SOTC encoded UWB-IR in the AWGN and the ISI-free UWB channels. Since the asymptotic analysis is only applicable to the medium-to-high SNR range, a semi-analytical bound is proposed to predict system performance at low SNR. Finally, we analyze the tradeoff among system throughput, BEP and transmission range for both RC and SOTC encoded UWB-IR systems.

A. Effective Free Distance

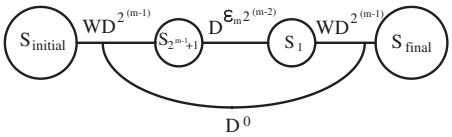

Fig. 1. Simplified diagram for all enumerations of input weight 2

We employ the input-output weight enumerating function (IOWEF) to obtain an closed-form expression of $d_{\text{free-eff}}$. Thanks to the special structure of the SOCC with orthogonal outputs, the effective augmented state diagram can be reduced to a state transition diagram, based on which all possible paths of input weight 2 can be calculated for given m.

Fig. 1 shows the simplified diagram for SOCC using the orthogonal branch metrics, where W and D are polynomials whose degrees represent the weights of the input and the output sequences, respectively. To calculate the enumerator function for the minimum weight codewords corresponding to input weight 2 and its compound error paths, we consider a shift register with memory m. Let d_{m1} be the minimum weight error sequence and d_{mi} with $i \neq 1$ be the compound error sequences. We have

$$d_{mi} = 2^m + i\epsilon_m 2^{m-2}, \tag{10}$$

where $i \in \{1, 2, \cdots\}$. For SOCC with the primitive feedback polynomial, $d_{\text{free-eff}}$ is given as

$$d_{\text{free-eff}}(m) = \min[d_{mi}] = 2^{m-2}[4 + \epsilon_m], \tag{11}$$

where ϵ_m captures the effect of the output weight increase during the intermediate stages as a function of m. ϵ_m can be iteratively computed by the following equation with $\epsilon_1 = 0$.

$$\epsilon_m = \epsilon_{m-1} + 2^{m-1}. \tag{12}$$

B. AWGN Channel

The asymptotic average upper bound on BEP of a Turbo Code in AWGN for medium to high SNR is given as [8]

$$P_b(e) = \sum_{w=1}^{N} W^w A^{PCC}(w, Z)\big|_{Z=\exp\left(\frac{1}{N_s}\frac{-E_b}{N_0}\right)}, \tag{13}$$

1-4244-0357-X/06/$20.00 ©2006 IEEE
This full text paper was peer reviewed at the direction of IEEE Communications Society subject matter experts for publication in the IEEE GLOBECOM 2006 proceedings.

where N is the interleaver size, w is the weight of the input sequence and A^{PCC} is the conditional IOWEF of the equivalent turbo code in a PCCC configuration. For a uniform interleaver analysis, $A^{PCC}(w,Z)$ is given by [8]

$$A^{PCC}(w,Z) \sim \frac{w!}{\eta_{max}} N^{2\eta_{max}-w}[A(w,Z,\eta_{max})]^2, \quad (14)$$

where $A(w,Z,n)$ is the parity enumerating function with n-concatenated error events caused by input weight w. η_{max} is the maximum number of error events in the trellis caused by input weight w.

For SOTC with recursive SOCC, the asymptotic performance is determined by the parity enumerating function $A(2,Z,1)$ that gives the parity weight of all possible paths generated by input weight $w=2$. Calculation of $A(2,Z,1)$ for a given SOCC involves all enumerations of input weight $w=2$. Based on Fig. 1 and (11), all possible enumerations for input weight $w=2$ in the indeterminate Z can be obtained as

$$A(2,Z,1) = \sum_{p=0}^{\infty} Z^{z_{min}+p\epsilon_m 2^{m-2}} = \frac{Z^{z_{min}}}{1-Z^{\epsilon_m 2^{m-2}}}, \quad (15)$$

where $z_{min} = d_{free}(m) - 2$.

Using (13)-(15), we have the asymptotic BEP for SOTC with a uniform interleaver as

$$P_b(e) \le \sum_{k=1}^{\lfloor \frac{N}{2} \rfloor} \binom{2k}{k} N^{-1} \frac{(Z^{2+2z_{min}})^k}{(1-Z^{\epsilon_m 2^{m-2}})^{2k}}\Big|_{Z=\exp\left(\frac{1}{N_s}\frac{-E_b}{N_0}\right)}. \quad (16)$$

Thus, a large N_s increases the length of the SOTC orthogonal outputs of the trellis branches, which is effectively translated into a SOTC processing gain with BEP monotonic in N_s.

C. UWB Channel

To derive the asymptotic bound in UWB channels, we first compute the pairwise error probability (PEP) of the coded sequence. We consider turbo codes as equivalent block codes of length $M = N_s N$ with N being the interleaver length and ignoring the trailing bits to terminate the constituent codes to zero state due to large interleaver length assumption. The probability of error in a coded sequence is computed with reference to the all zero coded sequence. Let $\boldsymbol{c}_i$ be the $M \times 1$ coded sequence with $\boldsymbol{c}_0$ as the all zero coded sequence. The corresponding BPSK modulated codedword sequence is x_i where $x_i \in \{-1,1\}$ and $x_i = 2c_i - 1$ with $c_i \in \{0,1\}$. Given the channel model in (2) and the RAKE correlation mask in (5), the first bit output from RAKE is given as

$$r_0 = x_0 E_g \sum_{l=0}^{L-1} \alpha_l^2 + \sqrt{E_g} \sum_{l=0}^{L-1} \alpha_l n_l^0, \quad (17)$$

where $n_l^0 = \langle n(t), g(t-\tau_i)\rangle$ is the inner product between $n(t)$ and $g(t-\tau_i)$. Let $\tilde{n}_0 = \sqrt{E_g}\sum_{l=0}^{L-1}\alpha_l n_l^0$, where $\tilde{n}_0$ has zero mean and variance given as

$$\sigma_{\tilde{n}_0}^2 = E_g \sigma^2 \sum_{l=0}^{L-1} \alpha_l^2. \quad (18)$$

where $\{\alpha_l\}$ is the subset of $\{\alpha_{n,k}\}$.

Collecting the RAKE output of all bits of the coded sequence in an ISI-Free channel the PEP can be shown as

$$P_e(\boldsymbol{c}_0 \to \boldsymbol{c}_i|\boldsymbol{\alpha}) \le \exp\left(-\frac{E_b}{N_s N_0} d \sum_{l=0}^{L-1} \alpha_l^2\right), \quad (19)$$

where d is the hamming distance between the pair of codewords and $\boldsymbol{\alpha} = [\alpha_0, \cdots, \alpha_{L-1}]^T$ is the collected vector of channel impulse response and L is the number of RAKE fingers. The unconditional pairwise error probability is $P_e(\boldsymbol{c}_0 \to \boldsymbol{c}_i) = E_{\boldsymbol{\alpha}}\{P_e(\boldsymbol{c}_0 \to \boldsymbol{c}_i|\boldsymbol{\alpha})\}$, the closed form expression of which is non-trivial to evaluate due to log-normal distribution of channel amplitudes and hence we proceed with the conditional pairwise error probability.
Let $\tilde{P}_e(\boldsymbol{c}_0 \to \boldsymbol{c}_i|\boldsymbol{\alpha})$ be the pairwise error probability in (19) without the hamming weight d. Finally, replacing Z in (16) with the conditional PEP $\tilde{P}_e(\boldsymbol{c}_0 \to \boldsymbol{c}_i|\boldsymbol{\alpha})$, we have the average analytical bound on the conditional error probability

$$P_b(e|\boldsymbol{\alpha}) \le \sum_{k=1}^{\lfloor \frac{N}{2} \rfloor} \binom{2k}{k} N^{-1} \frac{(Z^{2+2z_{min}})^k}{(1-Z^{\epsilon_m 2^{m-2}})^{2k}}\Big|_{Z=\tilde{P}_e(\boldsymbol{c}_0 \to \boldsymbol{c}_i|\boldsymbol{\alpha})}. \quad (20)$$

To conclude, the asymptotic performance bound in AWGN is given by $E_{\boldsymbol{\alpha}}\{P_b(e|\boldsymbol{\alpha})\}$, where $E_{\boldsymbol{\alpha}}\{\cdot\}$ is the expectation operator with respect to $\boldsymbol{\alpha}$. Since the closed-form expression in (20) is non-trivial, we evaluate the asymptotic upper bound by resorting to numerical methods.

D. Semi-Analytical Bound (SAB)

The asymptotic analysis shown in Sec. III-B and Sec. III-C is only applicable to the medium-to-high SNR value (E_b/N_0) [5]. For low SNR analysis, one can either resort to the iterative convergence analysis using EXIT charts or the simple bound based on IOWEF of the code. Inspired by [9], we propose a simple but effective semi-analytic method to predict the system performance for low SNR.

Thanks to the ISI-free assumption, the signal at each RAKE finger undergoes an independent flat fading. From (17), we can easily show that the effective SNR for a particular realization of $\boldsymbol{\alpha}$ is given by

$$SNR_{\text{eff}} \approx \frac{1}{N_s}\frac{E_b}{N_0}\sum_{l=0}^{L} \alpha_l^2. \quad (21)$$

Similar to [9], we approximate the BEP value conditioned on given $\boldsymbol{\alpha}$, $P_{e,\text{eff}}(SNR_{\text{eff}}|\boldsymbol{\alpha})$, with the BEP at SNR_{eff} obtained in the AWGN channel. Next, the semi-analytical BEP is computed by averaging $P_{e,\text{eff}}(SNR_{\text{eff}}|\boldsymbol{\alpha})$ over a sufficient number of channel realizations as

$$P_{e,SAB} = E_{\boldsymbol{\alpha}}\{P_{e,\text{eff}}(SNR_{\text{eff}}|\boldsymbol{\alpha})\}. \quad (22)$$

By exploiting the BEP curve in AWGN together with (21) and (22), we can easily predict the BEP performance for any given multipath channel. However, being different from [9], our analysis is applied to coded systems. Since coded systems have the optimal performance in AWGN, the semi-analytical BEP obtained in (22) corresponds to the performance upper bound with perfect interleaving in fading channels. In the sequel, we refer this semi-analytical bound as SAB.

1-4244-0357-X/06/$20.00 ©2006 IEEE
This full text paper was peer reviewed at the direction of IEEE Communications Society subject matter experts for publication in the IEEE GLOBECOM 2006 proceedings.

E. Effect of N_s

Here, we investigate the effect of N_s on system throughput for a given distance and a specified BEP. The average transmit power is constrained by the following inequality

$$P_{t_{\text{avg}}} \leq \tau_d \cdot P_{max}, \tag{23}$$

where $\tau_d = \frac{\tau_g}{T_c}$ is the pulse duty cycle with τ_g being the pulse duration and $P_{max} = \int_{f_1}^{f_2} P(f)df$ is the maximum allowed transmit power with $P(f)$ being the power spectral density of the frequency band over $[f_1, f_2]$. The propagation loss in the free space is a function of distance ℓ and frequency f of the following form

$$L(\ell, f) = (4\pi\ell f)^2 / c^2. \tag{24}$$

The average received signal power can be obtained from (23)-(24) and reads

$$P_{r_{\text{avg}}} \leq \tau_d \left(\frac{c}{4\pi}\right)^2 \frac{P_{max}}{\ell^2} \frac{f_2 - f_1}{f_2 f_1} \tag{25}$$

Equating the *received* energy to noise ratio with the *target* energy to noise ratio, we have

$$\frac{P_{r_{\text{avg}}} N_s T_c}{N_o (f_2 - f_1)} = M_L \left(\frac{E_b}{N_0}\right)_{\text{target}} \left(\frac{1}{(f_2 - f_1)}\right), \tag{26}$$

where M_L is the link margin. Substituting (25) into (26) yields

$$M_L \left(\frac{E_b}{N_0}\right)_{\text{target}} \leq \tau_d \left[\left(\frac{c}{4\pi}\right)^2 \frac{P_{max}}{\ell^2} \frac{f_2 - f_1}{f_2 f_1}\right] \left(\frac{N_s T_c}{N_0}\right). \tag{27}$$

Finally, we get

$$N_s \geq \ell^2 \left(\frac{16\pi^2}{c^2}\right) \left(\frac{f_2 f_1}{f_2 - f_1}\right) \left[\frac{N_0 M_L (E_b/N_0)_{\text{target}}}{T_c P_{max} \tau_d}\right]. \tag{28}$$

Since the bit interval time is T_s, the corresponding throughput is $R = 1/T_s = 1/(N_s T_c)$.

IV. Simulation Results

Computer simulations have been conducted to validate our analytical results. The SOTC decoder employs the Max-Log-Map/Min-Sum algorithm with an interleaver of size $N = 1024$. Unless otherwise specified, four iterations are performed in SOTC decoding. The BEP performance is averaged over 1000 blocks.

A. AWGN Channel

Fig. 2 shows the simulation results for SOTC- and RC-encoded systems with $N_s = 3$ and 7 in AWGN. Due to the orthogonality of the concatenated code, the system performance with SOTC improves monotonically with the increase of N_s. Note that the performance of RC is independent of N_s for a fixed E_b/N_0. Fig. 2 shows that SOTC with $N_s = 7$ has more than 8 dB improvement over RC at BEP of 10^{-6}. The asymptotic analytical upper bound computed from Eq. (16) is also shown against the simulation results. These asymptotic bounds are only useful in the medium-to-high E_b/N_0 range where simulation is not a practical means to measure system performance [8].

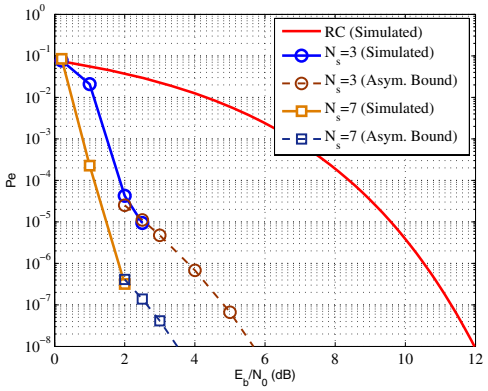

Fig. 2. SOTC and RC receivers in the AWGN channel.

B. IEEE 802.15.3a UWB Channel

We compare the performance of SRAKE for $N_s = 3, 7$ and $L_s = 10$ in Fig. 3. As shown in Fig. 3, the performance of SRAKE improves with N_s. The asymptotic bounds were obtained from (20). In contrast with the asymptotic bounds that are only applicable in the high E_b/N_0 region, the SAB derived from (22) can accurately predict system performance in the low E_b/N_0 region.

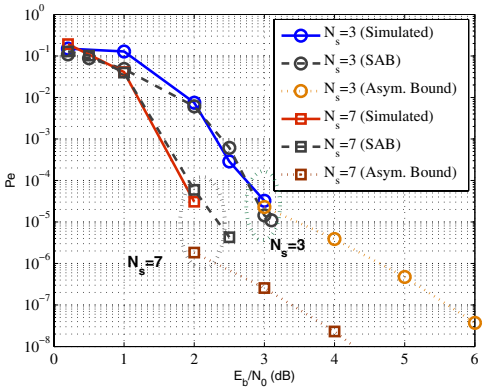

Fig. 3. The SRAKE performance in the UWB Channel with $L_s = 10$.

Fig. 4 shows the system performance as a function of the SRAKE finger numbers for different values of N_s. It is apparent that using more RAKE fingers for a given N_s can capture more paths, which results in better system performance. Furthermore, the system performance increases with N_s. However, Fig. 4 indicates that the performance improvement from $N_s = 7$ to $N_s = 15$ is much less than that from $N_s = 3$ to $N_s = 7$. This is mainly due to the fact that the energy per pulse for $N_s = 15$ is roughly half of that for $N_s = 7$. As a result, increasing the same number of RAKE fingers for $N_s = 15$ provides much less captured energy than that for $N_s = 7$. Hence, the marginal performance improvement diminishes as N_s increases.

C. Impact of N_s

In this experiment, we investigate the impact of N_s on the transmission distance and system throughput based on (28).

1-4244-0357-X/06/$20.00 ©2006 IEEE
This full text paper was peer reviewed at the direction of IEEE Communications Society subject matter experts for publication in the IEEE GLOBECOM 2006 proceedings.

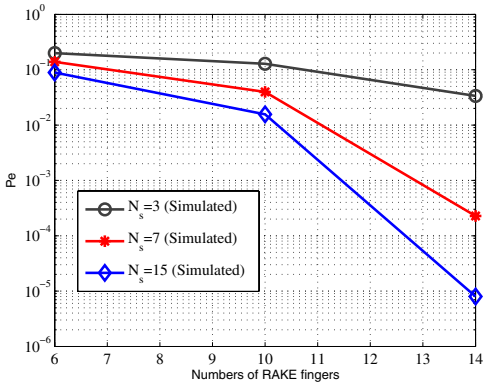

Fig. 4. S-RAKE system performance as a function of the finger number for different N_s at $E_b/N_0 = 1$ dB.

We primarily investigate the effect in AWGN with $T_c = 3$ ns and $\tau_g = 1$ ns for a link margin $M_L db = 7$.

Fig.5 shows the transmission distance as a function of N_s for a given target BEP of 10^{-6} in the AWGN channel. The corresponding $(E_b/N_0)_{\text{target}}$ for RC are calculated from closed form expression of BEP for RC and the $(E_b/N_0)_{\text{target}}$ for SOTC has been calculated from its performance curves for BEP Vs E_bN_0 using semi-analytical bound. It reveals that SOTC can achieve a significantly longer transmission distance than RC for the same throughput (*i.e.,* N_s). In particular, the improvement increases exponentially with N_s. However, a large N_s increases the number of trellis states, and subsequently the memory required in decoding.

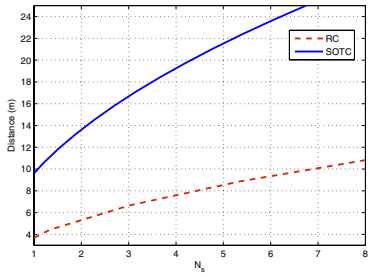

Fig. 5. Transmission distance as a function of N_s for a given BEP=10^{-6}.

We see from Fig. 5 that the SOTC-encoded system requires a much smaller N_s than the RC-encoded system to achieve the same transmission distance, which leads to higher throughput. This effect is further magnified in Fig. 6. In the ISI-free UWB channels, we have to increase the frame duration, T_c, to avoid interference from the adjacent symbols. As a result, the throughput in the ISI-free UWB channels depends on both N_s and T_c. Fig. 6 indicates that the RC receiver suffers a significant amount of throughput loss due to the increase of $T_c = 40$ ns . For the SOTC-encoded system, the adverse impact of a larger N_s on throughput is alleviated by the fact that SOTC with a larger N_s has better BEP performance. As a result, the SOTC-encoded system transmission range is much higher than the RC-encoded system in the ISI-free UWB channel for the same throughput and BEP.

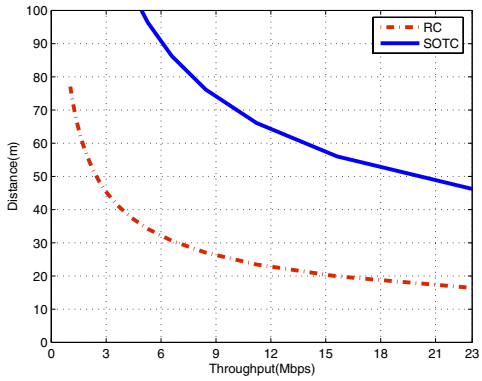

Fig. 6. Throughput as a function of the transmission distance in the ISI-free UWB channel for BEP=10^{-6}.

V. Conclusion

The performance of a DS-UWB system coded with SOTC in AWGN and ISI-free UWB channels was studied in this work. The SOTC scheme is attractive due to its low rate and low-decoding-complexity features. The asymptotic performance bounds for large SNR values were derived. Then, a semi-analytic method was proposed to predict the system performance at the low-to-medium SNR range. Through analysis and simulation, it was shown that the SOTC-encoded UWB system requires fewer pulses per information bit to achieve a given BEP than the conventional RC-encoded system, which leads to higher system throughput and/or a longer transmission range depending upon the application constraints..

References

[1] M. Z. Win and R. A. Scholtz, "Impulse radio: how it works", *IEEE Commun. Lett.*, vol. 2, no. 2, pp. 36–38, Feb. 1998.

[2] A.R. Forouzan, M. Nasiri-Kenari, and J.A. Salehi, "Performance analysis of time-hopping spread-spectrum multiple-acces systems: uncoded and coded systems", *IEEE Trans. on Comm.*, vol. 1, no. 4, pp. 671–681, Oct. 2002.

[3] N. Yamamoto and T. Ohtsuki, "Performance evaluation of adaptive internally turbo coded ultra wideband-impulse radio (AITC-UWB-IR) in multipath channels", *VTC2004 Fall, Los Angeles, CA*, vol. 2, pp. 1179 – 1183, Sep. 2004.

[4] U. Riaz, M.O. Pun, and C.-C. Jay Kuo, "Ultra-wide band impulse radio (UWB-IR) with super-orthogonal turbo codes (sotc)", *39th Asilomar*, vol. 49, no. 1, pp. 253–258, Nov. 2005.

[5] P. Komulainen and K. Pehkonen, "A low complexity superorthogonal turbo-code for CDMA applications", *Proc, IEEE PIMRC'96, Taipei*, vol. 2, pp. 369–373, Feb. 1996.

[6] "IEEE 802.15 WPAN high rate alternative PHY task group 3a (TG3a)", *http://www.ieee802.org/15/pub/TG3a.html*.

[7] A. Saleh and R. Valenzuela, "A statistical model for indoor multipath propagation", *JASC*, vol. 5, no. 2, pp. 128 – 137, Feb. 1987.

[8] S. Benedetto and G. Montorsi, "Design of parallel concatenated convolutional codes", *IEEE Trans. Com.*, vol. 44, no. 5, pp. 591–600, May 1996.

[9] A. Rajeswaran, V.S. Somayazulu, and J.R. Foerster, "RAKE performance for a pulse based UWB system in a realistic UWB indoor channel", *Proc. ICC*, vol. 5, pp. 28792883, 2003.

1-4244-0357-X/06/$20.00 ©2006 IEEE

This full text paper was peer reviewed at the direction of IEEE Communications Society subject matter experts for publication in the IEEE GLOBECOM 2006 proceedings.